

Influences of structure parameters on the detectivity of quantum dot infrared detectors

HONG ZHANG, YI ZHANG, X. SANG, C. YU, G. ZHOU, J. YUAN

Key Laboratory of Information Photonics and Optical Communications (BUPT),
Ministry of Education; Institute of Optical Communications and Optoelectronics, Beijing University of Posts and Telecommunications, Beijing 100876, China

To optimize the performance of quantum dot infrared detectors (QDIDs), influences of structure parameters on the detectivity are investigated. Effects of quantum dot (QD) density, doping levels, the number of QD layers and transverse distance between QD layers have been analyzed. Increasing densities of QD and donors can enhance the detectivity, but optimized detectivity needs a proper proportion between them. QDIPs exhibit optimized detectivity with the normalized QD density between 0.3~0.6, and the detectivity is sensitive to the transverse distances between QD layers when coupling is significant. The temperature sensitivity is discussed, the theoretical results agree well with the experimental results.

(Received May 20, 2009; accepted May 25, 2009)

Keywords: Quantum dot, Infrared detector, Doping

1. Introduction

In recent years, quantum dot infrared photodetectors (QDIPs) have been intensively investigated because of their potential applications in optical fiber communications, thermal imaging, etc[1]. Such a nano-structure is generally based on bound-to-continuum electron transitions in self-assembled GaAs quantum dots. The three-dimensional confinement of electrons in QDIPs leads to improved performances such as low dark current, intrinsic sensitivity to normal radiation, high operating temperature and high responsivity [2-5]. Both increased responsivity and reduced dark current will lead to higher detectivity which is important to estimate the performance of photodetectors. Recently, performances of the QDIP including the detectivity were experimentally analyzed[6]. Most of previous works mainly focused on the influence of the applied voltage, operating temperature and the concentration of donors, etc. Here, the influences of doping levels and different structure parameters on the detectivity of QDIPs to improve the performance are investigated.

2. Basic principle

The QDIP active region consists of a stacked-layer of quantum dots which are separated by wide-gap material

layers. The number of the QD layer is K . Each QD layer includes periodically distributed identical QDs (with the sheet density Σ_{QD}) doped with donors (with the sheet density Σ_D). Compared with its transverse size, the lateral size a of the QD is sufficiently large (so that the QD lateral area is equal to a^2). Such a structure insures that each QD has a large number of bound states and, therefore, is capable of accepting many electrons. The transverse size is much smaller than the spacing between the QD layers, L . Two heavily doped regions made of the same material as the barrier regions in which QDs are buried serve as the emitter and collector contacts. A schematic view of the considered QDIP structure is shown in Fig. 1.

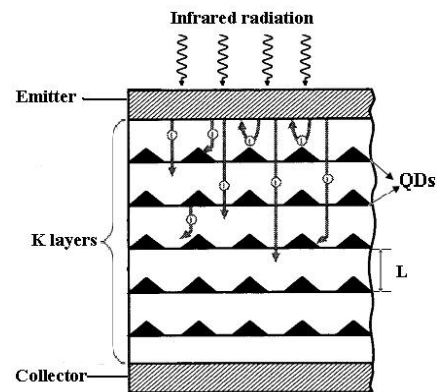


Fig. 1. Schematic of the QDIP structure.

The small transverse size provides the existence of a single energy level associated with the quantization in this direction. The flattened shape of large QDs ensures every QD has a large number of bound states so that it can capture a great average number of electrons, which makes the charges of QDs in the same QD layer are approximately the same. So the current arising under applied voltage depends on the potential distribution in the QDIP active region. Considering that the average number of electrons captured in each QD is the same, the total thermoexcitation and photoexcitation rate can be presented in the form [7]:

$$G^{dark} = g_{\Sigma_{QD}} K \exp\left(-\frac{\epsilon_l}{k_B T}\right) \left[\exp\left(\frac{\pi \hbar^2 N}{m k_B T a^2}\right) - 1 \right] \quad (1)$$

$$\approx g_{\Sigma_{QD}} K \exp\left[\frac{(\pi \hbar^2 / m a^2) N - \epsilon_l}{k_B T}\right]$$

and

$$G^{ph} = \sigma I \Sigma_{QD} K N \quad (2)$$

In equations (1) and (2), g is the pre-exponential factor, ϵ_l is the ionization energy of the ground state in QDs, T is the temperature, k_B is Boltzmann constants, and m is the effective mass of electrons in QDs, \square is the photoescape cross section, I is the photon flux and N is the average number of electrons in each QD.

The detectivity of the QDIP for a thermally-limited detection can be expressed as:

$$D^* = \frac{G^{ph}}{2 \hbar \Omega I \sqrt{G^{dark}}} \quad (3)$$

where \hbar is the Planck constant, Ω is the photon frequency.

In the voltage range $k_B T \square eV < e(V_{QD} - V_D)$ where QDs are not totally filled, one can obtain:

$$N = N_{QD} \frac{(V + V_D)}{V_{QD}} \quad (4)$$

N_{QD} is the maximum number of electrons which can be accepted by each QD, V is the applied voltage. $V_{QD} = eK(K+1)\Sigma_{QD}LN_{QD}/2\epsilon_0\epsilon_r$, $V_D = eK(K+1)\Sigma_D L/2\epsilon_0\epsilon_r$ are the characteristic voltages[8], where e is the electron charge, ϵ_0 is the Vacuum dielectric constant and ϵ_r is the relative dielectric constant.

With Equations (1)-(4), the following equation can be achieved:

$$D^* = \frac{\sigma N_{QD}(V + V_D)}{2 \hbar \Omega V_{QD}} \sqrt{\frac{K \Sigma_{QD}}{g}} \exp\left[\frac{\epsilon_l - \pi \hbar^2 N_{QD}(V + V_D)/(m a^2 V_{QD})}{2 k_B T}\right] \quad (5)$$

3. Results and discussions

The maximum of the detectivity can be obtained with equation (5) when

$$\Sigma_{QD} = 2 \pi \hbar^2 (V + V_D) \epsilon_0 \epsilon_r / k_B T m a^2 e K (K + 1) L \quad (6)$$

From Equations (6) and (4), the following equivalent condition should be met

$$\frac{k_B T m a^2}{\pi \hbar^2} = \frac{V + V_D}{V_{QD}} = \frac{N}{N_{QD}} \quad (7)$$

As $N < N_{QD}$, the condition can be used to restrict the QD lateral size a with,

$$a < \sqrt{\frac{\pi \hbar^2}{m k_B T}} \quad (8)$$

Equation (8) places a limitation to the QD lateral size a at a certain voltage. Although QD of larger size can accept more electrons, large QD will limit the QD sheet density, which leads to low absorption efficiency of QDIPs. Dark current can be reduced by small QDs in which the activation energy is close to the QD ionization energy. And it is evident that smaller QDs will increase QD density, which is a good choice to improve the detectivity. The distance of neighbouring QDs and base-to-height ratio (b/h) must be noticed about small QDs[9]. Large distance or low b/h will change the quantum level and energy band, leading to an unpredictable situation of QDIPs.

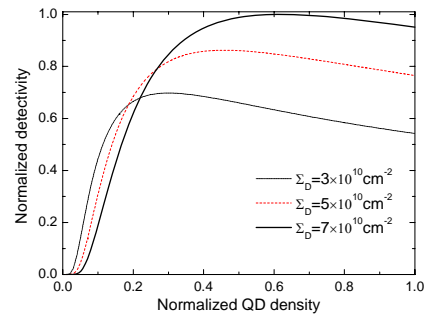


Fig. 2. Normalized detectivity versus normalized QD density of QDIPs with different doping levels.

Fig. 2 shows the normalized detectivity as a function

of the normalized QD density $\Sigma_{QD}a^2$ for QDIPs with different doping levels calculated using Equation (5) at $T=80K$, $V=0.5V$. In the calculations we assumed that $K=20$, $L=20nm$, $a=15nm$, $\epsilon_r=12$, $m=4\times 10^{-29}g$.

As the QD density increases, the detectivity reaches its maximum. With the rising of the QD density, donors provide enough electrons at first so that the process of emission and capture of mobile carriers in QDs and emitter will run in a good way. On the contrary, as the QD density keeps increasing, QDIP at a lower doping level becomes in short of the electrons, leading to the detectivity decrease. As mentioned above, the augmentation of QD density can't be arbitrary because of the restriction by QD size and technique of fabrication. On other hand, heightening of the doping level is a way to improve the performance of the QDIPs. As predicted[9,10], doping in the same layer with QDs will disturb the distribution of the potential and have an inferior effect. Because ionized dopants appear at too high doping level will lead to leakage current path in barriers and wet layer.

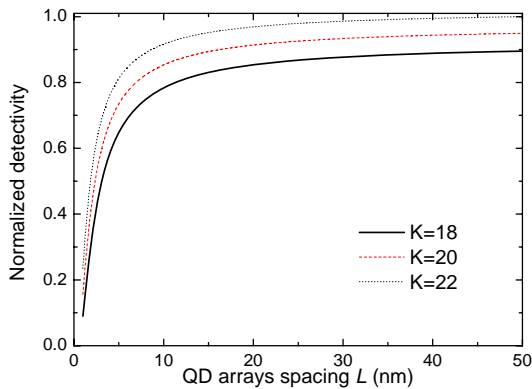


Fig. 3. Normalized detectivity as a function of the QD arrays spacing L .

The structure parameters play an important role in the same way in the QDIPs. Fig. 3 demonstrates the effect of different QD array spacing L and the number of QD layers on the normalized detectivity. The detectivity shows a sharp increase when L is smaller than 20nm and becomes saturated for L larger than $\sim 25nm$. When two QD layers are close enough in transverse direction, QDs are tightly coupled. As a result, electrons activated from one QD are easily reabsorbed by the other, which constricts the excitation rate and undermines the detectivity as shown in Fig.3 for $L < 10nm$. When L is larger than 25nm, the bottleneck of coupling is removed, and the increase in L shows little influence on the detectivity.

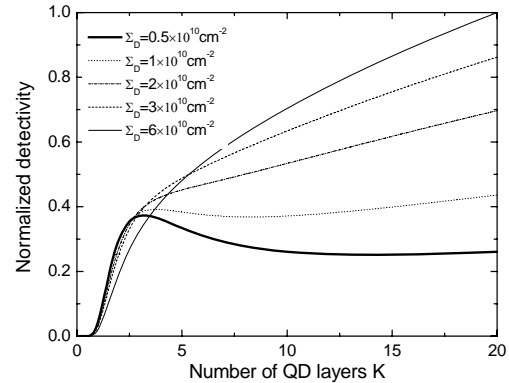


Fig. 4. Influence of the number of QD layers on the normalized detectivity.

On the other hand, increasing the number of K gives rise to both the rate of thermal excitation and photoexcitation. But the ratio of G^{ph} and $(G^{dark})^{1/2}$ increases with K as a whole. However, too many layers of stacking will lead to the degradation of the quality due to the accumulation of internal strain with increasing number of QD layers[11]. So the number of QD layers can't increase without an end in realistic applications. And the thickness of QDIPs will affect the detectivity anyway.

Moreover, as shown in Fig. 4, detectivity increases significantly only when doping density meets certain level, since lack of electrons will limit detectivity at slight doping level. Improvements can be made by close-pack distribution of QDs in different layers. Electrons penetrate one QDs layer through the "puncture" of the potential between QDs have larger probability to be absorbed by QDs in the next layer. In this way, thermoexcitation rate will decrease while photoexcitation rate will keep at the same level with fewer QDs layers. Hence, better detectivity can be achieved.

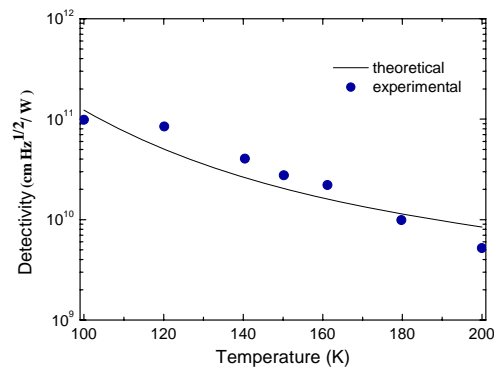


Fig. 5. The dependence of the detectivity on temperature.

We can also know that the confinement of temperature under condition (8), which means that the detectivity is sensitive to temperature in this model. High operating temperature will have a great impact on the detectivity of the QDIPs. Fig. 5 shows the calculated and experimental[12] detectivity-temperature characteristics of QDIP. It reveals a good agreement with the comparison of both the theoretical and experimental results. The detectivity declines nearly two orders of magnitude as temperature increases from 100K to 200K.

4. Conclusions

We have investigated the influences of some structure parameters on the detectivity of QDIPs in order to optimize its performance. As analyzed above, increasing densities of QD and donors can enhance the detectivity, but optimized detectivity needs a proper proportion between them. QDIPs exhibit optimized detectivity with the normalized QD density between 0.3~0.6, and the detectivity is sensitive to the transverse distances between QD layers when coupling is significant. At a proper doping level, detectivity increases with the increase of the number of QD layers without consideration of internal strain. In the end, the temperature sensitivity is demonstrated, which agrees well with the experimental results.

Acknowledgements

This paper is partly supported by the National Basic Research Program of China (2006CB921105), the Specialized Research Fund for the Doctoral Program of Higher Education(20070013001), Co-construction Program of Beijing Municipal Commission of Education (XK100130837) , Research Grant of BUPT.

References

- [1] S. D. Gunapala, S. V. Bandara, C. J. Hill, D. Z. Ting, J. K. Liu, S. B. Rafol, E. R. Blazejewski, J. M. Mumolo, S. A. Keo, S. Krishna, Y.-C. Chang, C. A. Shott, *Infrared Phys. Technol.* **50**, 149 (2007).
- [2] J. Campbell, A. Madhukar, *Proc. IEEE* **95**, 1815 (2007).
- [3] V. Ryzhii, I. Khmyrova, M. Ryzhii, V. Mitin, *Semicond. Sci. Technol.* **19**, 8 (2004).
- [4] X. Lu, M. J. Meisner, J. Vaillancourt, J. Li, W. Liu, X. Qian, W. D. Goodhue, *Electron. Lett.* **43**, 589 (2007).
- [5] B. S. Passmore, J. Wu, M. O. Manasreh, V. P. Kunets, P. M. Lytvyn, G. J. Salamo, *IEEE Electron. Device Lett.* **29**, 224 (2008).
- [6] S. Chakrabarti, *IEEE Photon. Technol. Lett.* **17**, 178 (2005).
- [7] V. Ryzhii, I. Khmyrova, V. Mitin, M. Stroschio, M. Willander, *Appl. Phys. Lett.* **78**, 3523 (2001).
- [8] P. Martyniuk, S. Krishna, A. Rogalski, *J. Appl. Phys.* **104**, 034314 (2008).
- [9] H. C. Liu, *Opto-Electron. Rev.* **11**, 1 (2003).
- [10] V. Ryzhii, *Semicond. Sci. Technol.* **11**, 759 (1996).
- [11] R. Oshima, H. Komiyama, T. Hashimoto, H. Shigekawa, Y. Okada, *IEEE 4th World Conference on Photovoltaic Energy Conversion, Conference Record of the 2006, Waikoloa, HI*, **1**, 158 (2006).
- [12] S. Chakrabarti, A. D. Stiff-Roberts, P. Bhattacharya, S. Gunapala, S. Bandara, S. B. Rafol, S. W. Kennerly, *IEEE Photon. Technol. Lett.* **16**, 1361 (2004).

*Corresponding author: xzsang@gmail.com